

Photoluminescence of photonic polaritons

A. Ridolfo, S. Stelitano, S. Patanè, S. Savasta, and R. Girlanda

Dipartimento di Fisica della Materia e Ingegneria Elettronica, Università di Messina, Salita Sperone 31, I-98166 Messina, Italy

(Received 15 October 2009; revised manuscript received 30 November 2009; published 17 February 2010)

We study the photoluminescence properties of a monolithic optical device constituted by two coupled microcavities. A thin film of tetrakis(4-methoxyphenyl)porphyrin was embedded in one of these two cavities, whereas the other one is a dielectric structure coupled to the first one by means of a LiF/ZnS Bragg mirror. This optical device is the photonic analog of a microcavity embedded quantum well in the strong-coupling regime. We report on photoluminescence spectra obtained exciting incoherently the bottom cavity by its embedded organic layer and detecting light either from the bottom or the top cavity. A quantum statistical approach for interacting quantum systems in the strong-coupling regime reproduces with very good agreement the experimental results.

DOI: [10.1103/PhysRevB.81.075313](https://doi.org/10.1103/PhysRevB.81.075313)

PACS number(s): 78.55.-m, 71.20.Rv, 42.50.Ct, 78.67.Pt

I. INTRODUCTION

Optical microcavities (MCs) enable the resonant confinement of light to small volumes. Devices based on optical microcavities are already a key feature for a wide range of applications and studies.¹ When quantum emitters are coupled to a microcavity mode,² it is possible to realize important quantum optical effects and quantum information processing tasks, such as control of spontaneous emission, controlled coherent coupling, and entanglement of distinguishable quantum systems.³

In the past few years, much attention has been paid to optical microcavity structures with embedded active organic molecules.^{4–8} In this frame, organic materials are interesting due to their large exciton oscillator strengths and binding energies. These properties lead to a stronger interaction with the cavity mode and stable, strongly coupled states at room temperature.⁹ Organic materials offer great potential for a wide range of applications in both linear and nonlinear optics. Hence the special features and the flexibility of the organic molecules make them a very interesting candidate for the development of high-efficiency optoelectronic and photonic devices.^{10,11} Motivated by the success of single-cavity quantum electrodynamics experiments, the focus has recently moved to the exploration of applications and of the rich physics promised by quantum-optical systems in multicavity devices (see, e.g., Ref. 12). Different research groups have analyzed the light-matter interaction in multiple semiconductor coupled MCs (Ref. 13) and optical devices have been developed.^{14,15} The possibilities of active-passive configurations of such systems are almost limitless, including laser oscillators, directional switching of lasers, and a range of optical and electro-optic switches.¹⁶ Parametric oscillation in a monolithic semiconductor triple MC with signal, pump, and idler waves propagating along the vertical direction of the nanostructure has been demonstrated.¹⁵

In this paper, we study both experimentally and theoretically the photoluminescence (PL) properties of a monolithic organic based optical device constituted by two coupled MCs. The PL spectra from this coupled structure display two narrow peaks despite only one cavity (b) contains an active layer weakly coupled to the cavity mode. The presence of

two peaks of comparable height in the emission spectrum originates from the coupling of the two cavities. These emission peaks arise from the photonic analog of cavity polaritons. Cavity polaritons result from quantum wells (QW) excitons strongly coupled to cavity photons. Polariton PL arises after the incoherent pumping of one subsystem (QW excitons), detecting quanta from the other one (escaping cavity photons). Analogously, in the present device, we can detect light (PL_a) from the passive top cavity (a) while pumping the bottom cavity (b) by exciting the incoherent PL of the embedded active organic layer. However in contrast to the cavity polaritons, we can also pump and probe the same subsystem (PL_b) (the bottom cavity with the embedded organic layer). By this way it is possible to achieve a more complete characterization of the strong coupling between two subsystems and a more complete test of the theoretical models.

The study of the incoherent emission properties of cavity embedded quantum systems is also useful for understanding the emission properties of electroluminescent devices. In contrast theoretical studies are mainly concentrated on the reflectivity properties (see, e.g., Refs. 8 and 17). Electroluminescent devices based on organic thin films are attractive for their low-voltage operating, low power consumption, ease of fabrication and low cost.¹⁸ White organic light-emitting diodes (OLEDs) have drawn much attention due to their potential applications in full color displays with the help of color filters, in backlight for light crystal displays (LCDs), and eventually in solid-state lighting sources.^{19–21} A number of strategies have been reported to control the color purity. The improvement of the emitting properties in terms of light extraction and color purity needs a device architecture modeling. Coupled microcavity structures offer an efficient chance of tailoring the spectral properties of the emitted light. Hence theoretical modeling of light emission after incoherent excitation in strongly coupled systems with a reliable predicting character can be useful for the development of novel optoelectronic devices. The appropriate modeling of PL in coupled systems requires the correct description of the interplay between incoherent pumping (optical pumping at higher energy or even current injection) and decay resulting in a mixed quantum steady state. Here we compare the experimental results with a recently developed quantum statistical approach for interacting quantum systems in the strong-

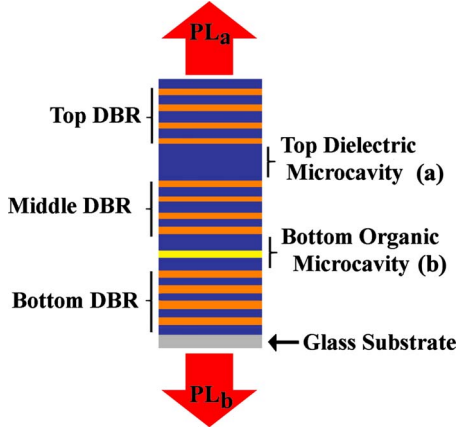


FIG. 1. (Color online) Schematic picture of the coupled microcavity structure.

coupling regime.²² This approach was initially developed to study the PL properties of a single quantum dot (QD) strongly coupled to a microcavity. We apply this theoretical framework to the case of incoherently pumped coupled microcavities. We find that the model provides PL spectra which are in excellent agreement with the experimental data. In particular we fit the PL_a data and use the fit parameters as input to calculate the PL_b signal without using any other fit procedure or free parameters. The calculation procedure is fully reversible, i.e., it is possible to fit the PL_b and calculate the PL_a . The impressive agreement with both PL_a and PL_b data demonstrates the ability of the theoretical model to fully catch the physics of the energy transfer between two strongly coupled subsystems under incoherent excitation. At the same time the excellent agreement between theory and experimental results is a clear signature of the good quality of the device.

II. STRUCTURE

The structure, schematically shown in Fig. 1, was grown by thermal evaporation in high vacuum (HV). The HV chamber was working at pressure below 4×10^{-6} Torr and it was equipped with three crucibles and a quartz based thickness monitor (Sycon—STM100). The films were deposited onto Corning 7059 glass substrates. The device consists of two microcavities coupled via a central distributed Bragg reflector (DBR). The ensemble is enclosed between a bottom and a top Bragg mirrors. The mirrors were made of quarter wavelength layers of lithium fluoride (LiF, $n_1=1.392$) and zinc sulfide (ZnS, $n_2=2.352$), used as low and high refractive index medium. Both LiF and ZnS were evaporated by using a tungsten boat at a deposition rate of about 0.5 and 0.1 nm/s, respectively. The top DBR contains four periods, the bottom DBR eight periods and the middle one is composed by 3.5 pairs.

Both cavities have a $\lambda/2$ optical length, but only the bottom (b) cavity contains, at its center, the active organic ultrathin layer, while the top (a) cavity is completely inorganic (LiF). The active layer consists of a 10-nm-thin film of tetrakis(4-methoxyphenyl)porphyrin (TMPP) whose molecu-

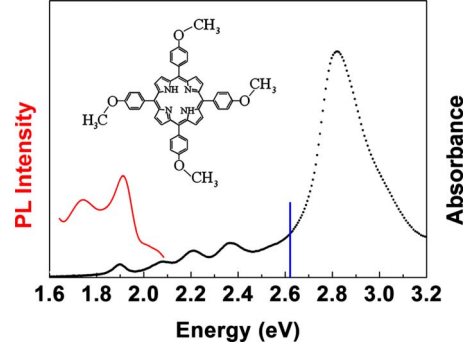


FIG. 2. (Color online) Absorption (dotted line) and PL spectra (continuous line) of the TMPP film. The vertical line indicates the energy of the exciting laser used for the PL experiments.

lar structure is reported in Fig. 2. The organic thin film deposition required a homemade MACOR based crucible, the organic layer was deposited at a rate of 0.05 nm/s.

The strong coupling of this double-microcavity structure has been demonstrated in Ref. 23, where normal-incidence optical reflectivity at room temperature was taken stepwise while growing the structure.

III. THEORY

In order to analyze the PL properties of the coupled double microcavity we exploit a quantum statistical approach for interacting quantum systems in the strong-coupling regime.²² We start considering a system of two coupled microcavities each of them can have an embedded layer of luminescent organic layer. Here we address the case where cavity photons and the organic excitations are in the weak-coupling regime, corresponding to the present experimental realization.

The master equation for the density matrix ρ of this system can be written as

$$\dot{\rho} = i[\rho, H_S] + \mathcal{L}_A^R + \mathcal{L}_B^R, \quad (1)$$

where the system Hamiltonian reads

$$H_S = \omega_a a^\dagger a + \omega_b b^\dagger b + g(a^\dagger b + ab^\dagger), \quad (2)$$

with g being the coupling strength between the two single mode cavities (with annihilation operator a and b , respectively) depending on the transmission of the central mirror. The superoperators \mathcal{L}_A^R and \mathcal{L}_B^R describe the interaction of the two cavity modes with reservoirs providing both damping and (when present) pumping mechanisms. Each of these terms consists of two contributions arising from two independent reservoirs: $\mathcal{L}_C^R = \mathcal{L}_C^{R1} + \mathcal{L}_C^{R2}$ ($C=A, B$). Transmission and diffraction losses of the cavity modes can be modeled, within a quasimode picture, as an effective coupling with a continuous ensemble of electromagnetic modes through the output mirrors.²⁴ When dealing with optical frequencies it can safely be regarded as a zero-temperature reservoir. The resulting Liouvillian term can be written as

$$\mathcal{L}_C^{R1} = \frac{\gamma_c^T}{2}(2c\rho c^\dagger - c^\dagger c\rho - \rho c^\dagger c), \quad (3)$$

where γ_c^T describes the transmission and diffraction losses of the cavity mode. The incoherent optical pumping originates from light emission from the optically active transitions of the cavity embedded organic layer providing the characteristic emission band (see Fig. 2). Such levels get populated after laser excitation of the absorption band at higher energy (Fig. 2). This mechanism can be described by an additional reservoir at a given effective temperature depending on the pumping rate.

We address the weak excitation regime where saturation effects are not present. In this case it is possible to describe the optically active transitions as an ensemble of harmonic oscillators coupled to the resonant light mode of the surrounding cavity. The interaction Hamiltonian can be written as

$$H_I = \sum_m g_m c^\dagger d_m + \text{H.c.}, \quad (4)$$

where $c=a$ or b , and d_m is the annihilation operator for the m th mode at energy ω_m . After the usual approximations leading to the master equation and neglecting the small Lamb and Stark shift terms,^{25,26} the corresponding Liouvillian term takes the form,

$$\mathcal{L}_C^{R2} = \frac{\gamma_c^L + P_c}{2}(2c\rho c^\dagger - c^\dagger c\rho - \rho c^\dagger c) + \frac{P_c}{2}(2c^\dagger \rho c - cc^\dagger \rho - \rho cc^\dagger), \quad (5)$$

where $P_c = \pi \sum_m g_m^2 \delta(\omega_c - \omega_m) \langle d_m^\dagger d_m \rangle$ describes the pumping rate of cavity c due to the incoherent emission from the excited levels of the organic molecules. The decay rate of the cavity mode is $\gamma_c^L = \pi \sum_m g_m^2 \delta(\omega_c - \omega_m)$. The resulting total Lindblad-like Liouvillian term for the cavity mode $\mathcal{L}_C^R = \mathcal{L}_C^{R1} + \mathcal{L}_C^{R2}$ can be written as

$$\mathcal{L}_C^R = \frac{\gamma_c + P_C}{2}(2c\rho c^\dagger - c^\dagger c\rho - \rho c^\dagger c) + \frac{P_C}{2}(2c^\dagger \rho c - cc^\dagger \rho - \rho cc^\dagger), \quad (6)$$

where $\gamma_c = \gamma_c^T + \gamma_c^L$ describes the total decay rate of the cavity photon number $\langle c^\dagger c \rangle$.

Starting from Eq. (1) a closed system of equations for the intracavity photon numbers $\langle c^\dagger c \rangle \equiv \text{Tr}[c^\dagger c \rho]$ can be easily obtained,

$$\frac{d}{dt} \langle a^\dagger a \rangle = -\gamma_a \langle a^\dagger a \rangle + 2g \text{Im} \langle a^\dagger b \rangle + P_a,$$

$$\frac{d}{dt} \langle b^\dagger b \rangle = -\gamma_b \langle b^\dagger b \rangle + 2g \text{Im} \langle b^\dagger a \rangle + P_b,$$

$$\frac{d}{dt} \langle a^\dagger b \rangle = \left[i(\omega_a - \omega_b) - \frac{\gamma_a + \gamma_b}{2} \right] \langle a^\dagger b \rangle + ig(\langle b^\dagger b \rangle - \langle a^\dagger a \rangle), \quad (7)$$

with $\langle b^\dagger a \rangle = \langle a^\dagger b \rangle^*$. We are interested in calculating the steady-state emission spectra: $S_c(\omega) = \lim_{t \rightarrow \infty} 2 \text{Re} \int_0^\infty \langle c^\dagger(t) c(t+\tau) \rangle e^{i\omega\tau} d\tau$. According to the quantum regression theorem,²⁵ two-time correlations $\langle A_n(t) A_m(t+\tau) \rangle$ follow the same dynamics of one-body correlation functions $\langle A_m(\tau) \rangle$ but with the one-time correlation $\langle A_n(t) A_m(t) \rangle$ as initial conditions. In our specific case the initial conditions are provided by the steady-state cavity occupations $\lim_{t \rightarrow \infty} \langle c^\dagger c \rangle$ and by $\lim_{t \rightarrow \infty} \langle a^\dagger b \rangle$. Hence we also need to derive the dynamics of one-body correlation functions:

$$\partial_t \langle a \rangle = -i\tilde{\omega}_a \langle a \rangle - ig \langle b \rangle,$$

$$\partial_t \langle b \rangle = -i\tilde{\omega}_b \langle b \rangle - ig \langle a \rangle, \quad (8)$$

where $\tilde{\omega}_c = \omega_c - i\gamma_c/2$. According to the input-output formulation of optical cavities,²⁴ the PL spectra obtained collecting the light escaping from the cavity a (or b) are proportional to $S_a(\omega)$ and $S_b(\omega)$, respectively. In particular the output field can be determined by the following relationship:

$$c_{\text{out}}(t) = c_{\text{in}}(t) + \sqrt{\gamma_c^T} c(t), \quad (9)$$

where $c_{\text{in}}(t)$ describes the input field operator. We are interested to the case where only one cavity has an embedded organic active layer ($P_a=0$). In this case, by applying the quantum regression theorem (see, e.g., Refs. 24 and 25), we obtain the following compact analytical expressions:

$$S_a(\omega) = \gamma_a^T \frac{P_b}{\sqrt{2\pi}} \frac{g^2}{|(\omega - \Omega_1)(\omega - \Omega_2)|^2}, \quad (10)$$

$$S_b(\omega) = \gamma_b^T \frac{P_b}{\sqrt{2\pi}} \frac{|\omega - \tilde{\omega}_a|^2}{|(\omega - \Omega_1)(\omega - \Omega_2)|^2}, \quad (11)$$

where Ω_i ($i=1,2$) are the complex Rabi resonances:

$$\Omega_{(1,2)} = \frac{\tilde{\omega}_a + \tilde{\omega}_b}{2} \mp \frac{1}{2} \sqrt{4g^2 + (\tilde{\omega}_a - \tilde{\omega}_b)^2}. \quad (12)$$

We observe that the input field operators do not provide any contribution to the PL spectra since we are considering the case where there is no input light field exciting resonantly the cavity, i.e., in the frequency range of interest where the spectrum is calculated.

As it can be easily inferred from the obtained expressions, the two spectra differ from each other significantly even at resonance $\omega_a = \omega_b$. It is also interesting to investigate the limit case of very small coupling $g \rightarrow 0$ or even $g \ll |\omega_a - \omega_b|$. In this case, from Eqs. (10) and (11), we obtain: $S_a(\omega) = 0$, and

$$S_b(\omega) = \gamma_b^T \frac{P_b}{\sqrt{2\pi}} \frac{4}{4(\omega - \omega_b)^2 + \gamma_b^2}. \quad (13)$$

In this limit, as expected, S_a goes to zero and S_b displays only one emission peak. As Eqs. (10) and (11) show (see also

Sec. IV), the coupling of the active cavity with an additional passive one can modify significantly the spectral properties of the emitted light. Equations (10) and (11) can be useful to design the double-cavity structure for tailoring the spectral properties of OLEDs and for the theoretical descriptions of PL measurements in double cavities. The procedure described in this section to derive Eqs. (10) and (11) can be easily generalized to the case of multiple cavities beyond two.

IV. PL: THEORY AND EXPERIMENT

The PL measurements were performed by exciting the cavity at $\lambda=473$ nm (2.62 eV) within the absorption band of the organic layer (see Fig. 2) with a diode-pumped solid-state (DPSS) laser operating in continuous wave mode with a power density of about 120 kW/m². We checked that lowering the input power density does not provide any appreciable spectral modification. The PL signal at longer wavelengths was collected by a lens that focused the light on the end face of a single-mode optical fiber. Finally the spectrum emitted by the MC was analyzed by a monochromator coupled to a charge coupled device detector. The measurements were carried out at room temperature. The PL spectra were obtained in two different conditions: first by collecting the light emitted from the top side of the cavity (PL_a); second collecting the light emitted from the bottom side of the sample (PL_b). As can be inferred from the theoretical analysis of the previous section, the system of two-coupled MCs can be viewed as the photonic analog of cavity polaritons resulting from QW excitons strongly coupled to cavity photons. PL from polaritons is obtained by pumping incoherently one subsystem (QW excitons) and detecting quanta from the other subsystem (outgoing cavity photons). In the strong-coupling regime what is measured are photons (originating from the radiative recombination of excitons) emitted at the energy of the new eigenmodes of the system (i.e., polaritons) and not at that of the uncoupled modes (i.e., neither at the energy of the uncoupled QW exciton nor at that of the cavity photon). The detected photons in PL experiments carry information intimately linked with the dual light-matter nature of polaritons.

Analogously, in the present device, we can detect photons from the passive top cavity while pumping incoherently the bottom cavity by the PL from the embedded active organic layer. In this case the bottom cavity (b) and the top one (a) play the role of QW excitons and cavity photons, respectively. However in contrast to excitonic polaritons this photonic system allows the direct measurement of quanta escaping from the subsystems a and b . Specifically we can excite incoherently the subsystem b and detect light escaping from both the two subsystems PL_a and PL_b . In this way a more complete characterization of the energy transfer between two strongly coupled subsystems after incoherent excitation can be gathered. This information can be used for comparison with theoretical results in order to check the adherence of the experimental spectra to theoretical predictions for strongly coupled systems.

The theoretical approach presented in Sec. III, allows us to calculate the PL spectra which can be obtained for the two

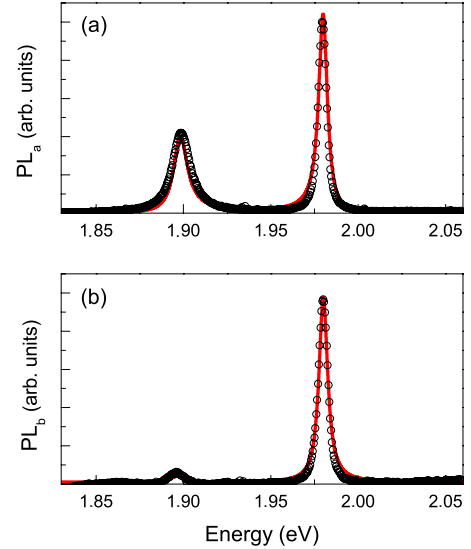


FIG. 3. (Color online) (a) Photoluminescence data (empty circles) and the corresponding theoretical fit (continuous line) for light escaping from the empty cavity (PL_a). (b) Photoluminescence data (empty circles) and the corresponding theoretical calculation (continuous line) for light escaping from the active cavity (PL_b).

cases. Figure 3(a) displays PL_a . The circles represent the experimental data collected at normal incidence from the side of the empty cavity, while the continuous line describes the best fit obtained by using Eq. (10). The obtained best fit parameters are: $\gamma_a=4.5$ meV, $\gamma_b=11$ meV, $\omega_a=1.962$ eV, and $\omega_b=1.916$ eV. The theoretical spectra have been obtained using a coupling strength $g=34$ meV. It has been previously obtained from the reflectivity spectra at normal incidence of the single and double structure taken stepwise while growing the device.²³ The obtained decay rate γ_a is significantly lower than γ_b . This difference reflects the difference between the reflectivity of the two external mirrors which provide the coupling of the two microcavities with the external modes. We notice that the obtained value of the coupling g satisfies the inequality $2g > \text{Max}(\gamma_a, \gamma_b)$, hence the system is in the strong-coupling regime. We also observe that the two cavities display a non-negligible detuning between their resonant energy; as a consequence the lower energy peak has a dominant contribution from the top cavity (a) while the narrower higher energy peak comes mainly from the bottom cavity (b). The quality factors of the two emission lines are about 160 and 320 and are compatible with standard transfer matrix calculations.

Figure 3(b) displays PL_b . The circles represent the experimental data collected from the side of the cavity with the embedded organic layer (bottom cavity). The continuous line shows the corresponding theoretical calculation according to (11). In particular after fitting the PL_a data [Fig. 3(a)] we use the obtained fit parameters as input to describe the PL_b signal without using any other fit procedure [Fig. 3(b)]. The agreement of the PL_b data with the theoretical calculation with no free parameters is rather impressive. The calculation procedure is fully reversible, i.e., it is possible to fit the PL_b and calculate the PL_a . The results show the ability of the theoretical model to fully catch the physics of the energy transfer

between two strongly coupled subsystem under incoherent excitation. On the other hand this very good agreement confirms the good quality of this hybrid active device and the strong coupling between the two coupled microcavities.

V. CONCLUSION

We studied experimentally and theoretically the photoluminescence properties of a monolithic optical device constituted by two coupled microcavities. A thin film of tetrakis(4-methoxyphenyl)porphyrin, was embedded in one of these two cavities, whereas the other one is a dielectric structure coupled to the first one by means of a LiF/ZnS Bragg mirror. This optical device, working at room temperature, is the photonic analog of a MC embedded quantum well in the strong-coupling regime. We report on the photoluminescence spectra obtained exciting incoherently the bottom cavity by its embedded organic layer and detecting light either from the bottom or the top cavity. In this way we were able to investigate

the strongly coupled system by exciting just one of the two subsystems and probing each of the two subsystems. Hence photonic polaritons provide an interesting tool to investigate the energetics of strongly coupled quantum systems. The experimental results have been compared with the theoretical predictions of a quantum statistical model developed for the analysis of PL from strongly coupling systems. The model is based on a master equation which includes the interaction between the two subsystems as well as their interactions with reservoirs providing both the decay and pumping mechanisms. The excellent agreement between the experimental data and the theoretical calculation shown in Fig. 3(b) demonstrates the predicting ability of the model. Theoretical modeling of light emission after incoherent excitation in strongly coupled systems with a reliable predicting character can be very useful for the design of light emitting optoelectronic devices based on cavity embedded organic active molecules.

-
- ¹K. J. Vahala, *Nature (London)* **424**, 839 (2003).
²R. J. Thompson, G. Rempe, and H. J. Kimble, *Phys. Rev. Lett.* **68**, 1132 (1992); H. Mabuchi and A. C. Doherty, *Science* **298**, 1372 (2002); J. M. Raimond, M. Brune, and S. Haroche, *Rev. Mod. Phys.* **73**, 565 (2001).
³A. Imamoglu, D. D. Awschalom, G. Burkard, D. P. DiVincenzo, D. Loss, M. Sherwin, and A. Small, *Phys. Rev. Lett.* **83**, 4204 (1999); P. Michler, A. Kiraz, C. Becher, W. V. Schoenfeld, P. M. Petroff, L. Zhang, E. Hu, and A. Imamoglu, *Science* **290**, 2282 (2000); K. Hennessy, A. Badolato, M. Winger, D. Gerace, M. Atatüre, S. Gulde, S. Fält, E. L. Hu, and A. Imamoglu, *Nature (London)* **445**, 896 (2007).
⁴M. S. Skolnick, V. N. Astratov, D. M. Whittaker, A. Armitage, M. Emam-Ismael, R. M. Stevenson, J. J. Baumberg, J. S. Roberts, D. G. Lidzey, T. Virgili, and D. D. C. Bradley, *J. Lumin.* **87-89**, 25 (2000).
⁵R. J. Holmes and S. R. Forrest, *Org. Electron.* **8**, 77 (2007).
⁶J. R. Tischler, M. S. Bradley, Q. Zhang, T. Atay, A. Nurmikko, and V. Bulovic, *Org. Electron.* **8**, 94 (2007).
⁷S. Stelitano, G. De Luca, S. Savasta, and S. Patanè, *Appl. Phys. Lett.* **93**, 193302 (2008).
⁸S. Stelitano, S. Savasta, S. Patanè, G. De Luca, and L. Monsù Scolaro, *J. Appl. Phys.* **106**, 033102 (2009).
⁹P. Pellandini, R. P. Stanley, R. Houdrè, U. Oesterle, M. Ilegems, and C. Weisbuch, *Appl. Phys. Lett.* **71**, 864 (1997).
¹⁰C. D. Müller, A. Falcou, N. Reckefuss, M. Rojahn, V. Wiederhirm, P. Rudati, H. Frohne, O. Nuyken, H. Becker, and K. Meerholz, *Nature (London)* **421**, 829 (2003).
¹¹S. Reineke, F. Lindner, G. Schwartz, N. Seidler, K. Walzer, B. Lüssem, and K. Leo, *Nature (London)* **459**, 234 (2009).
¹²C. Diederichs, J. Tignon, G. Dasbach, C. Ciuti, A. Lemaître, J. Bloch, Ph. Roussignol, and C. Delalande, *Nature (London)* **440**, 904 (2006).
¹³C. Diederichs and J. Tignon, *Appl. Phys. Lett.* **87**, 251107 (2005).
¹⁴A. Armitage, M. S. Skolnick, A. V. Kavokin, D. M. Whittaker, V. N. Astratov, G. A. Gehring, and J. S. Roberts, *Phys. Rev. B* **58**, 15367 (1998).
¹⁵D. Gerace, H. E. Tureci, A. Imamoglu, V. Giovannetti, and R. Fazio, *Nat. Phys.* **5**, 281 (2009).
¹⁶R. P. Stanley, R. Houdrè, U. Oesterle, P. Pellandini, and M. Ilegems, *Appl. Phys. Lett.* **65**, 2093 (1994).
¹⁷G. Panzarini, L. C. Andreani, A. Armitage, D. Baxter, M. S. Skolnick, V. N. Astratov, J. S. Roberts, A. V. Kavokin, M. R. Vladimirova, and M. A. Kaliteevski, *Phys. Rev. B* **59**, 5082 (1999).
¹⁸C. W. Tang and S. A. Vanslyke, *Appl. Phys. Lett.* **51**, 913 (1987).
¹⁹C. Hosokawa, M. Eida, M. Matsuura, K. Fukuoka, H. Nakamura, and T. Kusumoto, *Synth. Met.* **91**, 3 (1997).
²⁰S. Tao, Z. Peng, X. Zhang, and S. Wu, *J. Lumin.* **121**, 568 (2006).
²¹A. Misra, P. Kumar, M. N. Kamalasanan, and S. Chandra, *Semicond. Sci. Technol.* **21**, R35 (2006).
²²A. Ridolfo, O. Di Stefano, S. Portolan, and S. Savasta, arXiv:0906.1455 (unpublished).
²³S. Stelitano, G. De Luca, S. Savasta, L. Monsù Scolaro, and S. Patanè, *Appl. Phys. Lett.* **95**, 093303 (2009).
²⁴D. F. Walls and G. J. Milburn, *Quantum Optics*, 2nd ed. (Springer-Verlag, Berlin, 2008).
²⁵M. O. Scully and M. S. Zubairy, *Quantum Optics*, 1st ed. (Cambridge University Press, Cambridge, 1997).
²⁶C. W. Gardiner and P. Zoller, *Quantum Noise*, 2nd ed. (Springer, New York, 2000).